

Resonant detection of microwave radiation in a circular two-dimensional electron system with quantum point contacts

P. S. Dorozhkin, S. V. Tovstonog, S. A. Mikhailov, I. V. Kukushkin, J. H. Smet, and K. von Klitzing

Citation: *Appl. Phys. Lett.* **87**, 092107 (2005); doi: 10.1063/1.2035883

View online: <http://dx.doi.org/10.1063/1.2035883>

View Table of Contents: <http://aip.scitation.org/toc/apl/87/9>

Published by the [American Institute of Physics](#)



Small Conferences. BIG Ideas.

Applied Physics
Reviews

SAVE THE DATE!
3D Bioprinting: Physical and Chemical Processes
May 2–3, 2017 • Winston Salem, NC, USA

The background of the banner features a stylized, glowing blue and red network of lines, resembling a biological or physical structure, set against a dark blue background with light patterns.

Resonant detection of microwave radiation in a circular two-dimensional electron system with quantum point contacts

P. S. Dorozhkin,^{a)} S. V. Tovstonog,^{a)} S. A. Mikhailov,^{b)} I. V. Kukushkin,^{a)}
J. H. Smet,^{c)} and K. von Klitzing

Max-Planck-Institut für Festkörperforschung, Heisenbergstraße 1, D-70569 Stuttgart, Germany

(Received 21 March 2005; accepted 11 July 2005; published online 26 August 2005)

We demonstrate that a two-dimensional electron system with a circular mesa and with quantum point contacts along its periphery is an attractive device geometry for the resonant detection of electromagnetic radiation in the millimeter and microwave region. Its operation relies on the resonant excitation of edge magnetoplasmons and the quantum point contacts serve as rectifying elements. The resonant response can be tuned easily across a broad frequency range, for instance, by altering the magnetic field, the electron density or the radius of the disk shaped mesa. © 2005 American Institute of Physics. [DOI: 10.1063/1.2035883]

The frequency tunable detection of radiation in solids commonly exploits elementary excitations and the ability to externally control their properties. In quantum-well infrared photodetectors¹ and quantum-cascade-laser detectors,² the incident radiation stimulates *electronic* transitions between the ground and excited electron energy levels. An external applied electric field can alter the resonance frequency to some extent. In recently proposed *plasmon* detection schemes,^{3–6} radiation excites two-dimensional (2D) plasmons in a submicron field-effect transistor^{4,5} or in a 2D electron system (ES) with a grating.⁶ Rectification due to asymmetric boundary conditions at source and drain, for instance, produces a dc photocurrent. Tuning the electron density shifts the resonance frequency.

Both detection schemes based on electronic transitions and plasmons face severe difficulties when reducing the operation frequency ω . Detectors based on interlevel transitions rely on a substantial population difference between the levels and, hence, only operate properly when the thermal energy kT is much smaller than the photon energy $\hbar\omega$. For frequencies of the order of 1 THz and less, this condition is only fulfilled at temperatures well below 4 K. Here k and \hbar are the Boltzmann and Planck constants. For plasmon detection, the above condition is irrelevant and replaced with $\omega\tau \gg 1$ instead. The momentum relaxation time τ drops rapidly with increasing temperature. As a consequence, the successful resonant detection of radiation using plasmons was so far only reported for frequencies higher than ~ 0.6 THz and temperatures of ~ 10 – 25 K (Ref. 4–6).

Recently, it has been demonstrated^{7,8} (see also Ref. 9) that the use of a special type of plasma waves in the 2DES—*edge magnetoplasmons*^{10,11} (EMPs)—offers the opportunity to extend the operation of plasmon based detectors to substantially lower frequencies as well as higher temperatures. Irradiation of a Hall bar quantum-well sample with microwaves induced a photovoltage (and a change of the longitudinal resistance), which oscillated as a function of an applied perpendicular magnetic field B . The amplitude and the period

of these oscillations carried information about the incident radiation power and its frequency. The edge magnetoplasmons are classical plasma waves observable at any value of $\omega\tau$,^{12,13} as long as the cyclotron frequency exceeds the momentum relaxation rate, $\omega_c\tau \gg 1$. The operation of an EMP-based spectrometer was demonstrated at frequencies as low as 20–50 GHz and for temperatures up to ≈ 80 K (Ref. 8).

In this letter, we put forward another approach for frequency selective, resonant detection of microwave radiation in a GaAs/AlGaAs heterostructure and we also provide an experimental proof of concept. It relies on the resonant excitation of EMPs and the downconversion of the ac fields to a dc signal via rectification in so-called quantum point contacts (QPCs).¹⁴

The starting point is a 2DES shaped into a disk with radius R as shown in Fig. 1. Two leads are attached to the disk on opposite sides via narrow constrictions or QPCs. This sample is placed in a uniform and perpendicular magnetic field and is irradiated with microwaves. The incident radiation induces charge density oscillations in the disk. Near the boundary, e.g., at point A' (or B') in Fig. 1, the ac electric potential can be written as^{12,15} $\sum_{\ell} V_{\ell}(A')e^{i\ell\theta - i\omega t}$, with the complex amplitudes

$$V_{\ell}(A') = \frac{V_{\ell}^{\text{ext}}}{1 - \omega_L^2 / \omega(\omega + \omega_c \text{sgn}\ell + i/\tau)}. \quad (1)$$

Here, $\omega_L = \alpha_L(2\pi n_s e^2 / m\kappa R)^{1/2}$ is the resonant plasmon frequency at $B=0$, ℓ is the angular momentum quantum num-

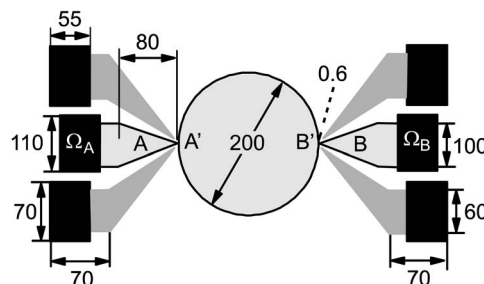


FIG. 1. The sample consists of a disk shaped 2DES contacted with a source and drain lead via constrictions with a lithographic width of $0.6 \mu\text{m}$. Two in-plane gates control the width of each constriction. All dimensions are in microns.

^{a)}Also at: Institute of Solid State Physics, Russian Academy of Sciences, Chernogolovka, 142432 Russia.

^{b)}Also at: Mid-Sweden University, ITM, Electronics Design Division, 851 70 Sundsvall, Sweden.

^{c)}Electronic mail: j.smet@fkf.mpg.de

ber, $L=|\ell|$, n_s is the 2D electron density, κ is the dielectric constant of the host semiconductor, and $V_\ell^{\text{ext}} \propto -RE_0$ is proportional to the amplitude E_0 of the incident electromagnetic wave. The numbers α_L are of order unity and can be evaluated numerically.¹⁶ Consider now the disk geometry with two QPCs attached to it (Fig. 1). If a dc voltage is applied across the ohmic contacts marked Ω_A and Ω_B , the current through the system will be determined mainly by the current-voltage (I - V) characteristics $I_{AA'}$ ($V_{AA'}=V_{A'}-V_A$) and $I_{BB'}$ ($V_{BB'}$) of the QPCs, which we assume here to be identical for simplicity. Under radiation, the potential $V_{A'}$ oscillates as a function of time with the amplitude determined by Eq. (1). The dc current through the disk acquires an additional photocontribution

$$I_{\text{ph}} \propto \frac{E_0^2 R^2}{4} \frac{d^2 I(V_{AA'})}{dV_{AA'}^2} \sum_{\ell} \left| 1 - \frac{\omega_L^2}{\omega(\omega + \omega_c \text{sgn} \ell + i/\tau)} \right|^{-2}, \quad (2)$$

proportional to the microwave power and the second derivative of the steady-state I - V characteristic of the QPC. The current I_{ph} has resonances at frequencies

$$\omega_\ell(B) = \sqrt{\omega_L^2 + (\omega_c/2)^2} - \omega_c \text{sgn} \ell / 2, \quad (3)$$

for which the edge ($\ell > 0$) and bulk ($\ell < 0$) magnetoplasmon modes in the disk are excited. Hence, these resonance positions can be controlled by the applied magnetic field, the size of the disk or, more conveniently, the electron density.

Experiments confirm this straightforward qualitative picture. The device geometry depicted in Fig. 1 was implemented on a GaAs/AlGaAs heterostructure with a dark electron density of $1.6 \times 10^{11} \text{ cm}^{-2}$ and a mobility of $6 \times 10^5 \text{ cm}^2/\text{V s}$. The 2DES was patterned into a disk shape and contacted via narrow constrictions with a width of $0.6 \mu\text{m}$ to source and drain leads on opposite sides. The conductance of each QPC was tuned with two in-plane gates. These in-plane gates were also formed out of the 2DES, but were separated from the disk and the leads by fully depleted trenches. The sample was placed in an oversized 16 mm waveguide near the maximum of the microwave electric field. Microwaves were produced with a backward wave oscillator with an output power up to 5 mW at the entrance of the waveguide. The microwave power was modulated at a frequency of 1 kHz. The measurements were carried out in liquid helium at 4.2 K.

The solid curves in Fig. 2 show dc I - V characteristics of the device, measured for two different gate voltages: $V_g=0$ and -7 V. At $V_g=-7$ V and small source-drain voltages V_{sd} , the QPCs are pinched off as the one-dimensional (1D) subbands of both constrictions are located above the electrochemical potentials of the disk and the leads.¹⁷ The threshold source-drain voltages V_{sd} at which current appears are ~ -0.35 and $+0.6$ V. The differential conductance rises from zero to hundreds of μS as the electrochemical potential in the source and the disk coincides with the bottom of the lowest 1D subband of the left and right constriction, respectively.¹⁷

Irradiation of the device with microwaves modifies the I - V characteristics especially near these threshold voltages (the dashed curve in Fig. 2). At $V_g=-7$ V, the microwave radiation decreases the threshold voltage. The photocurrent reaches a large absolute value near $V_{sd} \approx -0.35$ V and V_{sd}

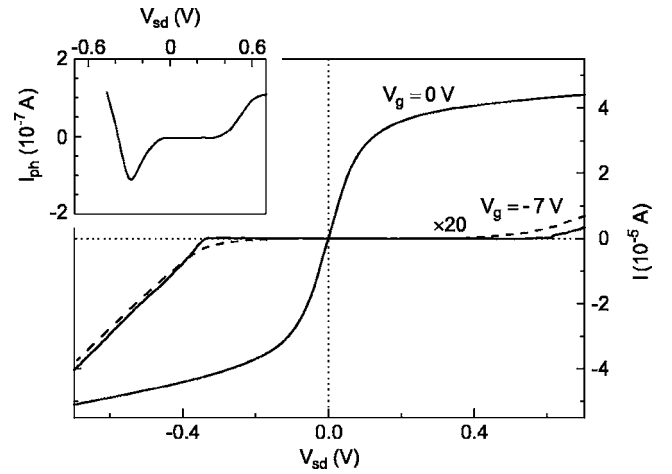


FIG. 2. dc I - V characteristics measured for different gate voltages $V_g=0$ and -7 V without (solid curve) and with (dashed curve) microwave irradiation ($40 \mu\text{W}$). Inset: The difference between the microwave induced and dark currents as a function of the source-drain voltage.

$= +0.55$ V (inset to Fig. 2). In the vicinity of these source drain voltages, the device displays the largest sensitivity to the incident microwave radiation. The amplitude of the microwave-induced photocurrent depends resonantly on the frequency and the magnetic field, in accordance with Eq. (2). Figure 3 displays the B -field dependence of the photocurrent for different microwave frequencies at $V_g=-7$ V and $V_{sd}=-0.35$ V. The I_{ph} curves show several pronounced maxima that move to lower magnetic fields upon increasing the microwave frequency. The positions of the resonances are insensitive to the gate voltage in the range from $V_g=-10$ to -5 V and are plotted in Fig. 4 (symbols). Different symbols correspond to different values of the gate voltage V_g . The solid curves represent the magnetic field dependence of the EMP modes $\omega_\ell(B)$ with $\ell=1, 2$, and 3 as calculated from Eq. (3). The calculations were carried out as described in Ref. 16 with $n_s=1.6 \times 10^{11} \text{ cm}^{-2}$, $R=100 \mu\text{m}$, and $\kappa=(\kappa_{\text{GaAs}}+1)/2$

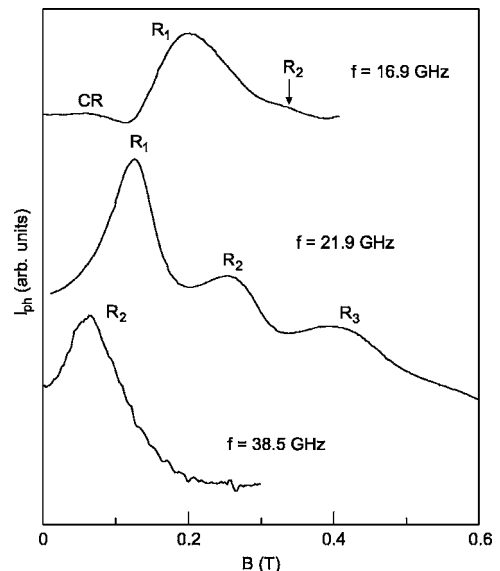


FIG. 3. Magnetic field dependence of the photocurrent I_{ph} at several microwave frequencies. The gate and the source-drain voltages were $V_g=-7$ V and $V_{sd}=-0.35$ V, respectively. CR marks the position of the cyclotron resonance. The index to each resonance peak R_ℓ refers to the angular momentum quantum number ℓ of the excited EMP.

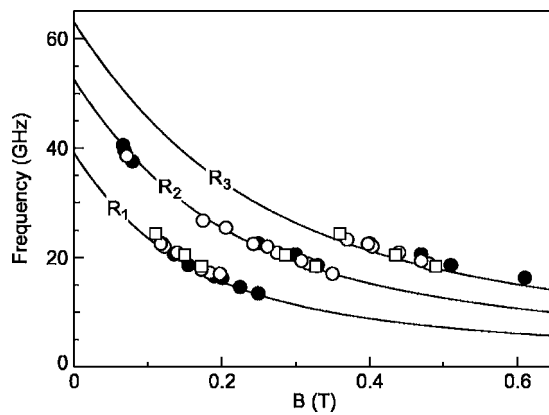


FIG. 4. Photocurrent resonance positions in experiment as a function of magnetic field. Different symbols correspond to different values of the applied voltage to the in-plane gates controlling the width of the constrictions: $V_g = -7$ V (open circles), -6 V (open squares), and -8 V (closed circles). Curves show the calculated dependencies, Eq. (3), for $\omega_\ell(B)$ with $\ell = 1, 2$, and 3.

$= 6.9$. The $B = 0$ plasmon frequencies, $\omega_L/2\pi$, are equal to 39.2, 52.6, and 63.1 GHz for $L = 1, 2$, and 3, respectively ($\alpha_{1,2,3} = 1.05, 1.41$, and 1.69). Note that no photoresponse resonance at frequencies corresponding to the bulk magneto-plasmon modes $\omega_{\ell < 0}(B)$ has been observed. The QPC detection scheme is sensitive mainly to the ac field near the boundary of the device (at points A', B' in Fig. 1). Hence, it is more susceptible to the edge modes than bulk modes.

We conclude, based on the excellent agreement between experiment and theory, that the observed photocurrent resonances are intimately related to the excitation of the three lowest EMP modes. We emphasize that the EMPs, activated when applying a moderate magnetic field, enhance the performance of plasmon based resonant detection techniques as their damping is not governed by the condition $\omega\tau \gg 1$. The device presented here as well as the device reported in Ref. 8, which is also based on EMPs, can be operated at temperatures up to at least 80 K. Both devices exhibit a comparable sensitivity of the order of 100–1000 V/W, but the present device excels in terms of its spectral resolution, in particular at frequencies below 20 GHz. Easy tunability of the resonance frequency, with the help of a backgate or by changing the disk geometry, contributes further to the attractiveness of this EMP-QPC technique for the resonant detection of elec-

tromagnetic radiation in the millimeter/terahertz region.

The authors acknowledge financial support from Max-Planck and Humboldt Research Grants, from the Russian Fund of Fundamental Research, INTAS, the Swedish Foundation for International Cooperation (STINT), and the BMBF through a Young Investigator Award on Nanotechnology.

¹See e.g., M. Graf, G. Scalari, D. Hofstetter, J. Faist, H. Beere, E. Linfield, D. Ritchie, and G. Davies, *Appl. Phys. Lett.* **84**, 475 (2004), and references therein.

²D. Hofstetter, M. Beck, and J. Faist, *Appl. Phys. Lett.* **81**, 2683 (2002).

³M. I. Dyakonov and M. Shur, *IEEE Trans. Electron Devices* **43**, 380 (1996).

⁴W. Knap, Y. Deng, S. Rumyantsev, J.-Q. Lü, M. S. Shur, C. A. Saylor, and L. C. Brunel, *Appl. Phys. Lett.* **80**, 3433 (2002).

⁵W. Knap, Y. Deng, S. Rumyantsev, and M. S. Shur, *Appl. Phys. Lett.* **81**, 4637 (2002).

⁶X. G. Peralta, S. J. Allen, M. C. Wanke, N. E. Harff, J. A. Simmons, M. P. Lilly, J. L. Reno, P. J. Burke, and J. P. Eisenstein, *Appl. Phys. Lett.* **81**, 1627 (2002).

⁷I. V. Kukushkin, M. Y. Akimov, J. H. Smet, S. A. Mikhailov, K. von Klitzing, I. L. Aleiner, and V. I. Fal'ko, *Phys. Rev. Lett.* **92**, 236803 (2004).

⁸I. V. Kukushkin, S. A. Mikhailov, J. H. Smet, and K. von Klitzing, *Appl. Phys. Lett.* **86**, 044101 (2005).

⁹B. Simović, C. Ellenberger, K. Ensslin, and W. Wegscheider, *cond-mat/0502350*.

¹⁰V. A. Volkov and S. A. Mikhailov, in *Landau Level Spectroscopy*, Modern Problems in Condensed Matter Sciences Vol. 27.2, edited by G. Landwehr and E. I. Rashba (North-Holland, Amsterdam, 1991), Chap. 15, pp. 855–907.

¹¹S. A. Mikhailov, in *Edge Excitations of Low-Dimensional Charged Systems*, edited by O. Kiricek (Nova Science, New York, 2000), Chap. 1, pp. 1–47.

¹²V. A. Volkov and S. A. Mikhailov, *Zh. Eksp. Teor. Fiz.* **94**, 217 (1988), [*Sov. Phys. JETP* **67**, 1639 (1988)].

¹³P. J. M. Peters, M. J. Lea, A. M. L. Janssen, A. O. Stone, W. P. N. M. Jacobs, P. Fozooni, and R. W. van der Heijden, *Phys. Rev. Lett.* **67**, 2199 (1991).

¹⁴B. J. van Wees, H. van Houten, C. W. J. Beenakker, J. G. Williamson, L. P. Kouwenhoven, D. van der Marel, and C. T. Foxon, *Phys. Rev. Lett.* **60**, 848 (1988).

¹⁵S. J. Allen, Jr., H. L. Störmer, and J. C. M. Hwang, *Phys. Rev. B* **28**, 4875 (1983).

¹⁶A. L. Fetter, *Phys. Rev. B* **33**, 5221 (1986).

¹⁷L. P. Kouwenhoven, B. J. van Wees, C. J. P. M. Harmans, J. G. Williamson, H. van Houten, C. W. J. Beenakker, C. T. Foxon, and J. J. Harris, *Phys. Rev. B* **39**, 8040 (1989).